Progress In Electromagnetics Research, Vol. 131, 275–292, 2012

A NOVEL RANGE-SPREAD TARGET DETECTION APPROACH FOR FREQUENCY STEPPED CHIRP RADAR

B. Liu* and W. Chang

School of Electronic Science and Engineering, National University of Defense Technology, Changsha, Hunan 410073, China

Abstract—This paper presents a novel range-spread target detection algorithm for frequency stepped chirp radar (FSCR) which transmits a chirp-pulse train with frequency stepped carriers. FSCR achieves high range resolution by synthetic wide-band technique, and its process includes intra-pulse matched filtering and pulse-to-pulse inverse discrete Fourier transform (IDFT) or wavelet transform. For FSCR, the high resolution range profile (HRRP) of a target is obtained by target extraction from overlapping HRRPs which is caused by oversampling. During the target extraction (sometimes called decorrelation), some strong scattering points of target echo are discarded, as the result, the signal-to-clutter ratio (SCR) might be reduced and the target detection capability is degraded. To solve this problem for FSCR, a novel detection algorithm without target extraction is addressed. The new algorithm based on the power spectrum of radar echo uses not only the amplitude information, but also the phase information of overlapping HRRPs of a target to improve the SCR, therefore, has significant performance. Moreover, the test statistic and the false alarm probability of the detector are derived, and the implementation procedure and the flow chart of the detection algorithm are designed. Finally, the detection performance is assessed by Monte-Carlo simulation, and the results indicate that the proposed algorithm has about 3dB detection improvement in SCR compared with the spatial scattering density generalized likelihood ratio test (SSD-GRLT) detector, and at the same condition, is superior to the integrator detector. In addition, the proposed algorithm is robust and easy to implement.

Received 25 June 2012, Accepted 16 August 2012, Scheduled 12 September 2012

* Corresponding author: Bo Liu (liubo19830120@163.com).

1. INTRODUCTION

High range resolution (HRR) radars use wideband waveforms to resolve individual scatterers within the target [1], presenting a high resolution range profile (HRRP) for use in target recognition or precise guidance [2–4]. Frequency stepped chirp radar (FSCR) is a kind of HRR radar and is widely used in recently years [5–8], for it can achieve high range resolution while still retaining the advantages of narrower instantaneous receiver bandwidth and lower analog-to-digital (AD) sampling rate [9]. Unlike instantaneous wideband radar, FSCR achieves high range resolution by synthetic wide-band technique. Its process includes intra-pulse matched filtering and pulse-to-pulse IDFT or wavelet transform, and then the HRRP of a target is obtained by target extraction from overlapping HRRPs which is caused by oversampling on chirp sub-pulse. The flow charts of signal processing for HRRP in instantaneous wideband radar and FSCR are showed in Figure 1(a) and Figure 1(b), respectively.

For HRR radars, the multiple scattering centers of the target may appear in a number of isolated range cells [10], so the target is usually named as range-spread target. The traditional point-like target detection schemes for low range resolution (LRR) radars may fail for HRR radars [11], therefore, it is necessary to develop range-spread target detection schemes. Many achievements have been made in range-spread target detection during the past decades [12–20] (and references therein). More precisely, range-spread target detection based on one transmitted pulse with Gaussian noise was investigated in [12–14]. In [12], a (N, k) range-spread target model was proposed and the effect of increased resolution on target detectability was studied, then the optimum detector for (N, k) target model was proposed relied on the generalized likelihood ratio test (GRLT). By comparing the performance of the integrator detector and the M out of N detector for (N, k) range-spread target in [13], Hughes indicated that the integrator detector was superior to the M out of N detector

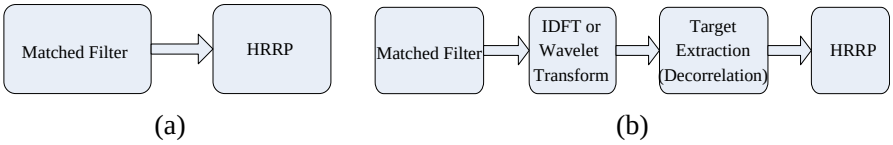

Figure 1. Signal processing for HRRP in instantaneous wideband radar and FSCR. (a) For instantaneous wideband radar. (b) For FSCR.

(sometimes called a binary integrator) in all cases except the case that the target was a point scatter. For using the knowledge of the spatial distribution of the desired target, a SSD-GLRT detection method was proposed in [14], and the simulation has indicated that SSD-GLRT detector is a robust detector when the scattering density parameter is known. In [15–20], based on the coherent target echoes, the adaptive constant false alarm rate (CFAR) detection of range-spread target modeled as rank-one signal in Gaussian noise has been studied. A range-spread target detection algorithm for frequency stepped radar was investigated in [21], where the HRRP was obtained by target extraction at the first step, and then the energy of the HRRP was accumulated by integrator to fulfill target detection.

However, the range-spread target detection methods proposed above are all based on HRRP of the target. For FSCR, during the target extraction to form HRRP, some strong scattering points of target echo might be discarded, as the result, the signal-to-clutter ratio (SCR) is reduced and the target detection capability is degraded. In this paper, a range-spread target detection algorithm without target extraction is addressed for a FSCR which is used in an anti-ship seeker. The new algorithm based on the power spectrum of radar echo uses not only the amplitude information, but also the phase information of the overlapping HRRPs of a target to improve the SCR. Initially, the echo model of a range-spread target for FSCR is analyzed, and a target detection model is built by investigating the time-frequency features of the overlapping HRRPs. Secondly, the detector based on the power spectrum of radar echo is presented, and the test statistic and the false alarm probability are derived. Moreover, the implementation procedure and the flow chart of the proposed detection algorithm are designed. Finally, the performance is verified by Monte-Carlo simulation which indicates that the proposed algorithm has about 3 dB improvement in SCR compared with the SSD-GRLT detector.

The paper is organized as follows. In Section 2, we state the problem to be addressed and build the radar echo model and target detection model. We derive the range-spread target detection algorithm based on the power spectrum in Section 3. In Section 4, the performance of the proposed detection algorithm is evaluated, and a comparison with previously detection schemes is made. At last, in Section 5, the conclusions and some hints for further research are given.

2. PROBLEM DESCRIPTION

2.1. Radar Echo Model

The transmitted signal of FSCR is expressed as:

$$s(t) = \sum_{i=0}^{M-1} A_i \cdot u_i(t) e^{j2\pi(f_0 + i\Delta f)t} \tag{1}$$

where $u_i(t) = rect[(t - iT_r)/T_p] e^{j\pi\mu(t-iT_r)^2}$, $\mu = B_c/T_p$, $u_i(t)$ is the i-th chirp sub-pulse, μ is the frequency slope of chirp sub-pulse,

A_i: amplitude of i-th chirp sub-pulse,

T_r: pulse repetition interval (PRI),

T_p: pulse width of chirp sub-pulse, and $T_p < T_r$,

B_c: band width of chirp sub-pulse,

f_0: nominal carrier frequency,

Δf: frequency step,

M: number of chirp sub-pulse.

According to the radar theory, the echo of a target is the convolution of the transmitted signal with the target range-scattering function. The range-scattering function of a static point-like target at the range of R_0 can be written as:

$$CF_0(t) = a_0 \cdot e^{j2\pi\varphi_0} \cdot \delta(t - 2R_0/c) \tag{2}$$

where a_0 is the amplitude, φ_0 the initial phase, and c the speed of light. Thus the range-scattering function of a static range-spread target can be expressed as:

$$CF(t) = \sum_v a_v \cdot e^{j2\pi\varphi_v} \cdot \delta(t - \tau_v) \tag{3}$$

where a_v, φ_v and τ_v are the amplitude, initial phase and delay of the v-th physical scatterer of the target in range cell, respectively. It is worth to note that $CF(t)$ is sensitive to the target's gesture and the radar observation angle. Assuming that $CF(t)$ is stationary during a coherent processing interval (CPI), the pulse compression result of the i-th chirp pulse for FSCR is given as:

$$\begin{aligned} y_i(t) \;=\; & \sum_v a_v \sqrt{\mu T_p^2}\, rect[(t - iT_r - \tau_v)/T_p] \\ & \cdot \sin c[\pi B_c(t - iT_r - \tau_v)] \cdot e^{-j2\pi\phi_v} \cdot e^{-j2\pi i\Delta f\tau_v}, \\ & i = 0, 1, \ldots, M-1. \end{aligned} \tag{4}$$

The sampling time in each PRI is T_G, and $T_p < T_G < T_r$. The sampling rate is f_s, sampling period $T_s = 1/f_s$, and $t = k \cdot T_s$. Therefore, the discrete pulse compression result of the i-th chirp pulse can be expressed as:

$$\begin{aligned} y_i(k) &= \sum_v a_v \sqrt{\mu T_p^2}\, rect[(kT_s - iT_r - \tau_v)/T_G] \\ &\quad \cdot \sin c[\pi B_c(kT_s - iT_r - \tau_v)] \cdot e^{-j2\pi\phi_v} \cdot e^{-j2\pi i \Delta f \tau_v}, \\ &\quad i = 0, 1, \ldots, M-1. \end{aligned} \tag{5}$$

$k = 0, 1, 2, \ldots, N-1$, N is the number of samples, and $N = T_G \cdot f_s$.

The high resolution matrix obtained by the IDFT of discrete pulse compression results in Equation (5) can be written as:

$$\begin{aligned} z(k,i) = IDFT[y_i(k), M] = |y_i(k)| \sum_v & \frac{\sin\ [\pi M \Delta f (\frac{i}{M\Delta f} - \tau_v)]}{M \sin[\pi \Delta f (\frac{i}{M\Delta f} - \tau_v)]} \\ & \cdot e^{-j2\pi(\varphi_v - \frac{M-1}{2}\Delta f \tau_v)} \cdot e^{-j2\pi(\frac{M-1}{2}\Delta f)\frac{i}{M\Delta f}} \\ & (k = 0, 1, \ldots, N-1; \quad i = 0, 1, \ldots, M-1.) \end{aligned} \tag{6}$$

The unambiguous time of high resolution profile is $1/\Delta f$, and the time resolution is $1/M\Delta f$ [22]. Assume that k_0 is the location of a target in coarse resolution domain, while $\{z(k_0, i), i = 0, 1, \ldots M-1.\}$ is a HRRP of the target. In Equation (6), the first phase term $e^{-j2\pi(\varphi_v - \frac{M-1}{2}\Delta f \tau_v)}$ is a constant, and the phase in the second phase term $e^{-j2\pi(\frac{M-1}{2}\Delta f)\frac{i}{M\Delta f}}$ is a linear function of i. Therefore, the HRRP of the target is an amplitude-modulated sinusoid signal with frequency $(M-1)\Delta f/2$, and the modulation envelope is $|y_i(k_0)|$. If there is relative movement between the target and FSCR, motion compensation is necessary before taking the IDFT to synthesize HRRP [23, 24].

A simulation of a range-spread target with four scattering centers is shown in Figure 2. Figure 2(a) shows the two-dimensional top view of $|z(k,i)|$. The horizontal is the coarse resolution axis, and the ordinate is the high resolution axis. The number of chirp sub-pulse $M = 32$. Figure 2(b) shows a HRRP of the target $\{|z(123,i)|, i = 0, 1, \ldots, 31.\}$. As can be seen, the four scattering centers of the range-spread target are clearly distinguished. Figure 2(c) shows the coarse resolution profile of the target $\{|y_0(k)|, k \in [100, 160]\}$. It can be seen that the four scattering centers of the target smear because the chirp sub-pulse has no enough band-width. Figure 2(d) shows a complex HRRP of the target $\{z(123,i), i = 0, 1, \ldots, 31.\}$, which is an amplitude-modulated sinusoid signal, and the modulation envelope is shown in Figure 2(b).

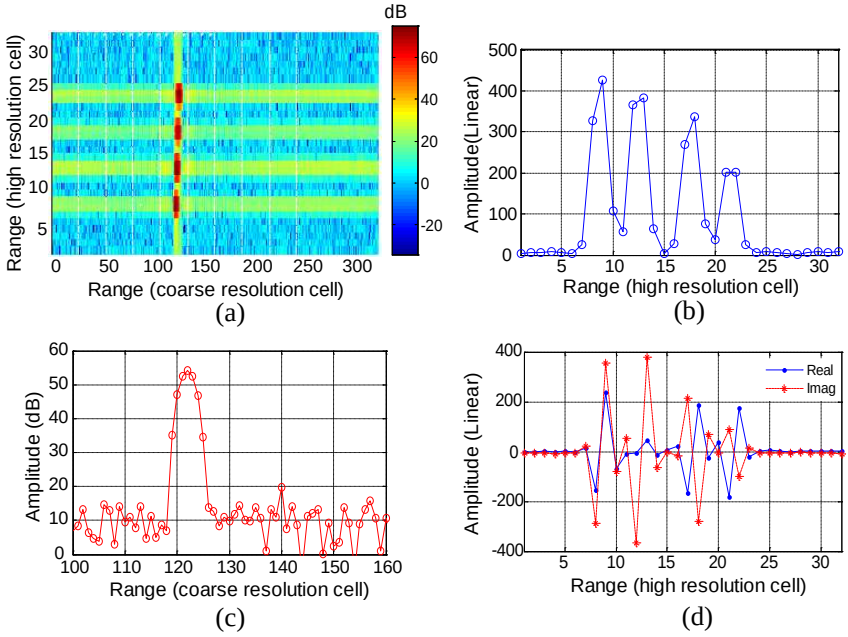

Figure 2. A range-spread target for FSCR. (a) Top view of the high resolution matrix. (b) HRRP of the target. (c) Coarse-resolution profile of the target. (d) Complex HRRP of the target.

2.2. Detection Model

The clutter, caused by ocean wave, is assumed to be much greater than the receiver thermal noise, thus thermal noise can be ignored [17, 25]. Meanwhile, the clutter is assumed to be Gaussian distributed with zero-mean, variance σ^2, homogeneous, and independent from range cell to range cell [12]. Moreover, assuming only one range-spread target in the area of coverage, each scatterer of the target independently follows the same Rayleigh amplitude distribution.

When receiving the chirp sub-pulse, the sampling frequency f_s should meet the Nyquist sampling theorem. In practice, f_s should satisfy the following formula [26]:

$$f_s > 1.5 f_N \tag{7}$$

The sampling interval $T_s = 1/f_s$, and the unambiguous time of a HRRP is $1/\Delta f$. Generally, $T_s < 1/\Delta f$, thus HRRP of the target can be obtained by each samples in the main lobe of sub-pulse compression (SPC) result. Therefore, there are usually redundant HRRPs for

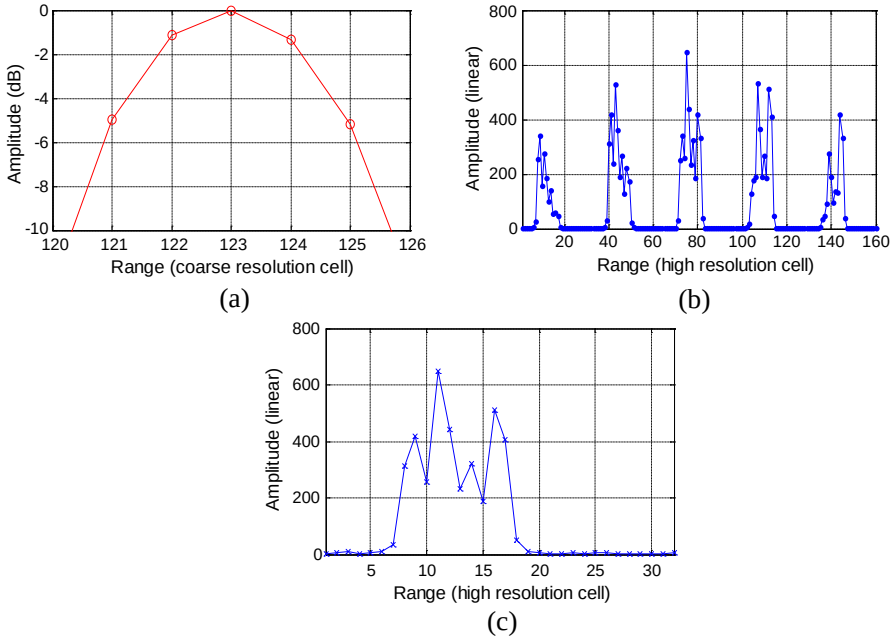

Figure 3. HRRPs obtained from five continuous samples within the main lobe of SPC result. (a) Five samples in the main lobe. (b) Redundant HRRPs. (c) Non-overlapping HRRP.

FSCR, which is the reason why target extraction is necessary to solve the problem of overlapped HRRPs.

Figure 3 shows the redundant HRRPs of a target for FSCR, and $M = 32$. As can be seen in Figure 3(a), there are five samples in the main lobe of SPC result. Along the coarse resolution axis, as shown in Figure 2, each of the five samples could generate a HRRP. If we make an arrangement of the five redundant HRRPs in the high resolution axis, a sequence of HRRPs can be formed, as shown in Figure 3(b). Target extraction is to get the non-overlapping HRRP of the target by removing the redundant range information contained in the strong scatterers in Figure 3(b). Many target extraction schemes have been proposed [27, 28], and a non-overlapping HRRP after target extraction is shown in Figure 3(c).

The strong scatterers which contain redundant range information of the target, as shown in Figure 3(b), are discarded during the target extraction. However, they are useful in target detection, because the energy of the discarded scatterers is part of the total energy returned from the target. The SCR increases if the energy

of these scatterers is integrated effectively, and the target detection performance is improved.

According to the radar theory [1], for a chirp pulse signal, the main lobe width of the pulse compression result is θ/B_c [9], where θ is the expansion factor of the weighting function, so the number of samples in the main lobe of sub-pulse compression result can be expressed as:

$$C = \text{int}[f_s \cdot \theta/B_c + 1] + 1 \tag{8}$$

where int[·] is round-off.

Setting a sliding-window of width $T_s \cdot (C-1)$ in the coarse That makes the integrated value of the largest window is chosen as the target detection window, denoted by W. The detection problem to be solved in W can be formulated in terms of the following binary hypotheses test:

$$\begin{array}{l} H_0 : Z_t = X_t \\ H_1 : Z_t = X_t + S_t \end{array} \qquad t = 0, 1, \ldots, C-1. \tag{9}$$

where Z_t, X_t, S_t are the received vector, clutter vector, and redundant HRRPs of the desired target, respectively, all M-dimension vectors with the t-th range cell in the coarse resolution domain. For the sake of simplicity, we make an arrangement in order of the high resolution domain, as shown in Figure 3(b). Therefore, Equation (9) can be rewritten as:

$$\begin{array}{l} H_0 : z_n = x_n \\ H_1 : z_n = s_n + x_n \end{array} \qquad n = 0, 1, \ldots, M \cdot C - 1. \tag{10}$$

where z_n, x_n, s_n are the received data, Gaussian complex clutter and target echo, respectively. To represent the overlapped HRRPs of a target, ultimately, the target detection model can be given by:

$$\begin{array}{l} H_0 : z_n = x_n, \quad n = 0, 1, \ldots, M \cdot C - 1. \\ H_1 : \begin{cases} z_n = s_{1n} + x_n, & n = 0, 1, \ldots, M-1. \\ z_n = s_{2n} + x_n, & n = M, M+1, \ldots, 2 \cdot M - 1. \\ \ldots \\ z_n = s_{Cn} + x_n, & n = (C-1)M, (C-1)M+1, \ldots, C \cdot M - 1. \end{cases} \end{array} \tag{11}$$

where s_{in} is the i-th redundant HRRP of the desired target in W.

3. DETECTOR DESIGN

Effective integration of energy returned from the desired target is the key in range-spread target detection [13]. For FSCR, the synthesis HRRP of a target has its own characteristics. Firstly, as shown in Figure 3, the synthesis HRRP of a target is redundant before target extraction. The target detection model in Equation (11) can be seen as

a multiple range-spread targets detection model, thus previous range-spread target detection algorithms based on single target may fail for FSCR. Secondly, envelops of the redundant HRRPs are similar to each other. This is because the redundant HRRPs obtained from continuous samples can be seen as a repetitive description of the same target almost at the same time. For instance, Figure 4 compares envelops of five redundant HRRPs of a target, where $M = 32$. Finally, the linear phases of the redundant HRRPs are identical, which can be seen from Equation (6). Consequently, effective energy integration of the redundant HRRPs which have similar envelops and identical linear phase is the key in target detection for FSCR.

As can be seen from Equation (6), the synthesis HRRP of a target is an amplitude-modulated sinusoid signal with frequency $(M-1)/2\Delta f$. Therefore, the center frequency of the power spectrum of a HRRP is $(M-1)/2\Delta f$. The redundant HRRPs have the similar envelops and identical linear phase, so approximately, the H_1 hypothesis in Equation (11) can be seen as a periodical extension of single HRRP, according to the signal processing theory [29], the power spectrum of the redundant HRRPs in Equation (11) is a discretization of the power spectrum of single HRRP. Therefore, the center frequency of the power spectrum of redundant HRRPs also is $(M-1)/2\Delta f$.

Figure 5 shows the power spectrums of single HRRP and the ordinal arrangement of the redundant HRRPs, where $M = 32$, $C = 5$, and the carrier frequency step $\Delta f = 6\,\text{MHz}$, so $(M-1)/2\Delta f = 93\,\text{MHz}$. Figure 5(a) shows the complex envelop of single HRRP whose power spectrum is shown in Figure 5(b). While Figure 5(c) shows the ordinal arrangement of five redundant complex HRRPs, the power spectrum is shown in Figure 5(d). It can be seen that Figure 5(d) is a discretization of Figure 5(b), and the center frequency of the power spectrums are both 93 MHz.

Accordingly, if we multiply the power spectrum of redundant HRRPs by a weighting function, the power of Gaussian clutter is

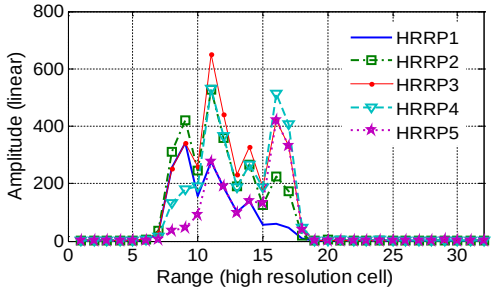

Figure 4. Envelops of five redundant HRRPs.

restricted, and then the energy of the target can be integrated by accumulating the product. According to Equation (11), the echo sequence can be written as:

$$E = \{z(n)|n = 0, 1, \ldots, L-1.\} \tag{12}$$

where $L = C \cdot M$. The power spectrum of E can be obtained by the discrete Fourier transform (DFT):

$$PS(k) = |Z(k)|^2 = \left| \sum_{n=0}^{L-1} z(n) \exp\left(-j2\pi \cdot \frac{kn}{L}\right) \right|^2, \quad k = 0, 1, \ldots L-1. \tag{13}$$

where $Z(k)$ is the DFT of $z(n)$, and $PS(k)$ is the power spectrum of $z(n)$. It should be stated that L, in practice, is not greater than 1024, so the calculation burden is acceptable.

The test statistic is defined as:

$$R = \frac{1}{L \cdot \sigma^2} \sum_{k=0}^{L-1} w(k) \cdot PS(k) \tag{14}$$

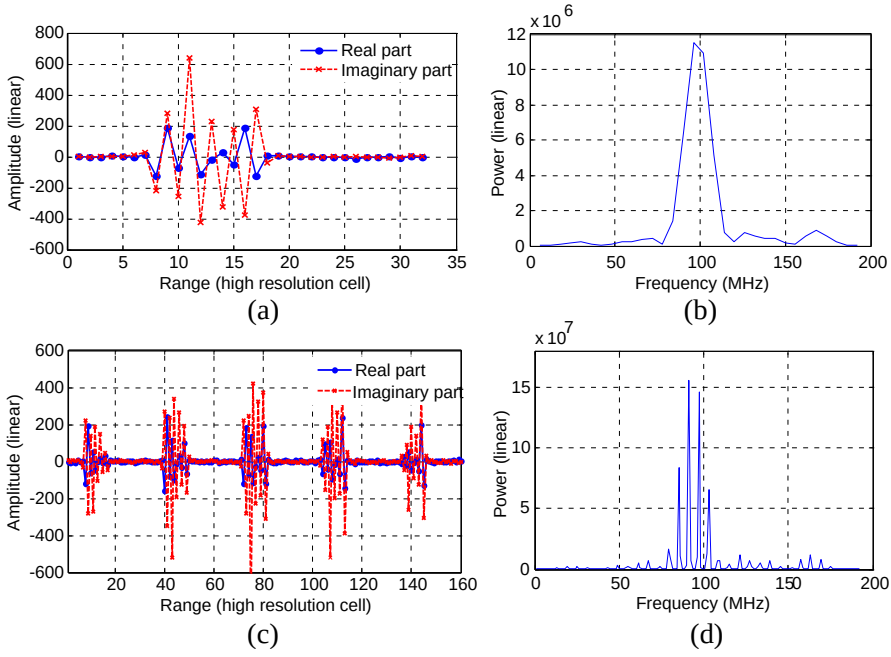

Figure 5. Power spectrums of target echo for FSCR. (a) Complex envelop of HRRP. (b) Power spectrum of single HRRP. (c) Arrangement of five redundant complex HRRPs. (d) Power spectrum of the redundant HRRPs.

where σ^2 is the variance of Gaussian clutter, and a maximum likelihood (ML) estimate of σ^2 can be obtained by the data out of the detection window W [12]:

$$\hat{\sigma^2} = \frac{1}{M(N-C)} \sum_{m \notin W} |z(m)|^2 \tag{15}$$

$w(k)$ is weighting function (such as Uniform weighting, Taylor weighting, and Hamming weighting). A uniform weighting function can be defined as [29]:

$$w(k) = \begin{cases} 1, & \frac{L-D}{2} \le k \le \frac{L+D}{2} - 1; \\ 0, & \text{else.} \end{cases} \tag{16}$$

where D is the width of the target's power spectrum, which is related to the physical property of the desired target and may be obtained by priori knowledge.

Under the H_0 hypothesis in Equation (11), $z(n) = x(n)$, $x(n) \sim N(0, \sigma^2)$, $Z(k) = DFT(z(n), L)$, while $Z(k) \sim N(0, L\sigma^2)$. So the test statistic R is in chi-square distribution with a freedom of $2D$ [11]. The probability distribution function (PDF) of R is expressed as [30]:

$$f(R) = \begin{cases} \frac{1}{2^D \Gamma(D)} R^{D-1} \exp(-\frac{R}{2}), & R > 0; \\ 0, & R \le 0. \end{cases} \tag{17}$$

where $\Gamma(\cdot)$ is the gamma function [30].

The false alarm probability (p_{fa}) is given by [12]:

$$p_{fa} = \int_T^{+\infty} \frac{1}{2^D \Gamma(D)} R^{D-1} e^{-R/2} dR \tag{18}$$

where T is the detection threshold and can be calculated when p_{fa} is known. As can be seen from Equation (18), the false alarm probability is independent of the external noise environment, hence Equation (14) gives a CFAR detector [17].

In summary, the range-spread target detection algorithm based on the power spectrum without target extraction for FSCR can be realized in the following six steps:

Step 1, calculate C by Equation (8), and then locate the target detection window W in the coarse resolution domain;

Step 2, make an ordinal arrangement of redundant HRRPs, and then the sequence which involves multiple range-spread targets is obtained.

Step 3, calculate the power spectrum of the sequence in step 2 by the DFT;

Step 4, estimate σ^2, D by Equation (15), get the test statistic R;

Step 5, calculate T by Equation (18) with a known false alarm probability;

Step 6, make a judgment:

$$H_1 : R \geq T \tag{19}$$

$$H_0 : R < T \tag{20}$$

Hypothesis H_1 denotes the presence of target in the test window, while H_0 denotes there is no target.

The flow chart of the proposed detection algorithm is shown in Figure 6.

4. PERFORMANCE ASSESSMENT

Under the H_1 hypothesis in Equation (11), closed-form expression for the probability of detection (p_d) is difficult to derive, hence the Monte Carlo method is carried out to evaluate the performance. The simulation parameters of FSCR are listed in Table 1. The parameters are selected according to [9]. Generally, the frequency step $\Delta f < B_c$, and the synthesis bandwidth $B_s = M \cdot \Delta f$ should satisfy the requirement of the radar system's range resolution.

Figure 7 shows the non-overlapping HRRPs of four range-spread targets simulated by computer for FSCR, where HRRPs of target 1, target 2, target 3, target 4 are shown in Figure 7(a), Figure 7(b),

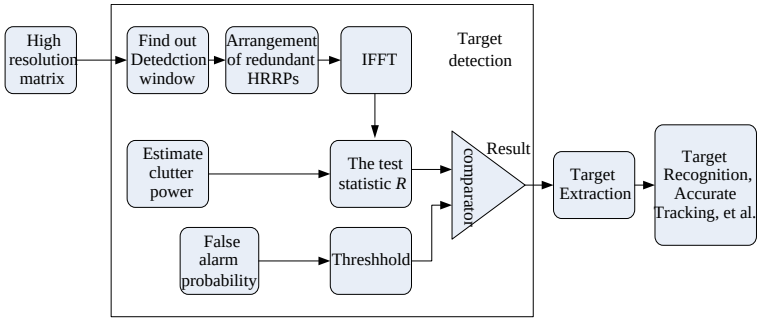

Figure 6. Flow chart of the proposed algorithm.

Table 1. Simulation parameters of FSCR.

Radar parameters	f_0	B_c	Δf	M	T_p	T_r	f_s
value	35 GHz	20 MHz	6 MHz	32	10 μs	200μs	40 MHz

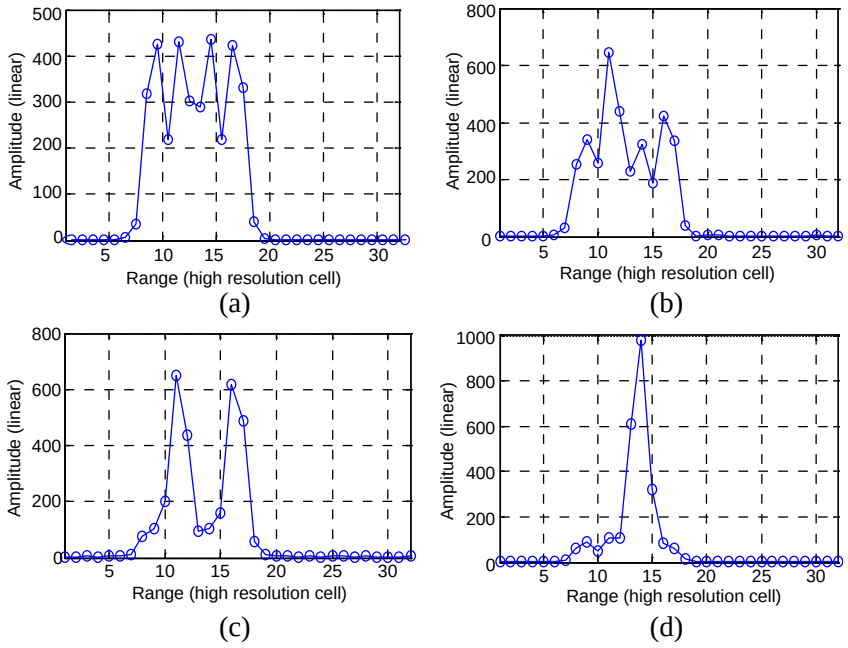

Figure 7. HRRPs of four target models. (a) Target 1. (b) Target 2. (c) Target 3. (d) Target 4.

Table 2. Target models, four scattering centers, and percentage of total energy in discrete scattering centers.

Model Number	Scattering centers number			
	1	2	3	4
1	1/4	1/4	1/4	1/4
2	1/6	1/2	1/6	1/6
3	0	1/2	1/2	0
4	0	0	1	0

Figure 7(c), and Figure 7(d), respectively. Each of the four targets has four scattering centers, and each HRRP of the four targets extends ten high resolution cells.

In the simulation, the total reflection energy from each of the four targets is identical, but the energy distributions among the scattering centers are different. Table 2 lists the percentage of total energy in discrete scattering centers of the four target models.

The mean signal-to-clutter ratio (SCR) is defined as:

$$SCR = 10\log_{10}\left[\frac{1}{n_c L \cdot \sigma^2}\sum_{k=0}^{L-1} w(k)\cdot PS(k)\right] \tag{21}$$

where n_c is the number of target's scatterers in redundant HRRPs. In this simulation, $n_c = 50$.

In the following, we present some results to demonstrate the effectiveness of the derived algorithm in detecting a range-spread target for FSCR. We compare the performance of the proposed algorithm with two detection schemes: integrator detector [12] without HRRP extraction and SSD-GRLT detector [14] after HRRP extraction. Gaussian clutter is generated by computer, where the variance is adjusted to SCR. We assume $p_{fa} = 0.0001$, and do 1000 independent trials at each SCR.

Figure 8 shows the detection performance of the three detectors for each of the four target models. Simulations for target 1, target 2,

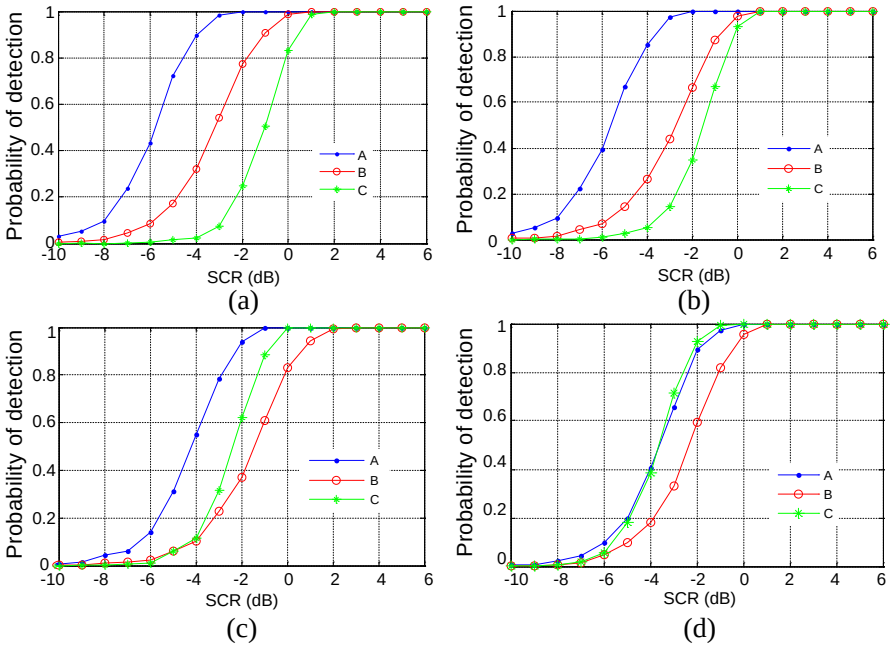

Figure 8. Detection performance of the three detectors for four target models, and $p_{fa} = 0.0001$. (a) P_d versus SCR for target 1. (b) P_d versus SCR for target 2. (c) P_d versus SCR for target 3. (d) P_d versus SCR for target 4. (A: Target detection algorithm based on the power spectrum; B: SSD-GRLT detector after target extraction; C: Integrator detector without target extraction.).

target 3 and target 4 are shown in Figure 8(a), Figure 8(b), Figure 8(c), and Figure 8(d), respectively.

We can make the following observations form Figure 8.

1) The proposed target detection algorithm has about 3 dB higher detection probability as compared with the SSD-GRLT detector after target extraction.
2) The integrator detector without target extraction has about 4 dB detection performance loss compared with the proposed algorithm for a range-spread target.
3) The detection performance of the integrator detector is almost the same as that of the proposed algorithm when the target energy concentrates on one scattering center.
4) The detection performance of the proposed algorithm has declined when the target energy distribution tends to concentrate on one scattering center, however, the loss is no more than 2 dB. Therefore, the target detection algorithm based on the power spectrum appears to be robust at different scatterers' distributions.

The reason for the proposed algorithm outperforming the SSD-GRLT detector after target extraction is that the energy of the redundant HRRPs of a target is integrated more effectively by the power spectrum based algorithm. For the integrator detector based on single range-spread target model, the H_1 hypothesis in Equation (11) is a multiple HRRPs model. While in estimation for the clutter parameters, some of the target energy is considered as clutter, so the SCR decreases and the detection performance degrades. When the target reflection energy concentrates on one single scattering center, the target becomes to be a point-like target, and the range-spread target model in Equation (11) can be regarded as a (N, k) range-spread target model [12], therefore, in this case, the performance of the integrator detector is almost as the same as that of the proposed algorithm.

5. CONCLUSION

In this paper, we present and assess a novel range-spread target detection scheme based on the power spectrum for frequency stepped chirp radar (FSCR). Firstly, a multiple range-spread targets detection model is built according to the time-frequency characteristics of redundant HRRPs of a target. Under this assumption, the range-spread target detection algorithm based on the power spectrum without target extraction is addressed. Moreover, the implementation

procedure and flow chart of the algorithm are designed. Monte Carlo simulation indicates that the proposed algorithm has about 3 dB higher detection probability as compared with the SSD-GRLT detector and is robust at different scatterers' distributions.

For FSCR, HRRP of a target is obtained by the target extraction which can be considered as incoherent integration of redundant HRRPs. Target extraction just uses the amplitude information of redundant HRRPs of a target, while the proposed detection algorithm based on the power spectrum is to make coherent integration to the target's redundant HRRPs. Namely, the proposed algorithm uses not only the amplitude information, but also the phase information of redundant HRRPs to improve the SCR. Therefore, it is superior to the detection algorithm after target extraction. It should be pointed out that the proposed algorithm applies to not only FSCR but also other synthesis wideband radars, such as frequency stepped pulse radar, frequency stepped continuous wave (FSCW) radar [9]. Further study on moving range-spread target detection for FSCR will be discussed in our next study.

REFERENCES

1. Barton, D. K. and S. A. Leonov, *Radar Technology Encyclopedia (Electronic Edition)*, Artech House, Boston, 1998.
2. Han, S.-K., H.-T. Kim, S.-H. Park, and K.-T. Kim, "Efficient radar target recognition using a combination of range profile and time-frequency analysis," *Progress In Electromagnetics Research*, Vol. 108, 131–140, 2010.
3. Calvo-Gallego, J. and F. Pérez-Martínez, "Simple traffic surveillance system based on range-Doppler radar images," *Progress In Electromagnetics Research*, Vol. 125, 343–364, 2012.
4. Huang, C. W. and K. C. Lee, "Application of ICA technique to PCA based radar target recognition," *Progress In Electromagnetics Research*, Vol. 105, 157–170, 2010.
5. Crowgey, B. R., E. J. Rothwell, L. C. Kempel, and E. L. Mokole, "Comparison of UWB short-pulse and stepped-frequency radar systems for imaging through barriers," *Progress In Electromagnetics Research*, Vol. 110, 403–419, 2010.
6. Park, S. H. and H. T. Kim, "Stepped-frequency ISAR motion compensation using particle swarm optimization with an island model," *Progress In Electromagnetics Research*, Vol. 85, 25–37, 2008.
7. Zhai, W. and Y. Zhang, "Application of super-SVA to stepped

chirp radar imaging with frequency band gaps between subchirps," *Progress In Electromagnetics Research B*, Vol. 30, 71–82, 2011.

8. Park, S.-H., H.-T. Kim, and K.-T. Kim, "Stepped-frequency ISAR motion compensation using particle swarm optimization with an island model," *Progress In Electromagnetics Research*, Vol. 85, 25–37, 2008.
9. Wehner, D. R., *High-resolution Radar*, Artech House, Boston, 1995.
10. De Maio, A., "Polarimetric adaptive detection of range-distributed targets," *IEEE Transactions on Signal Processing*, Vol. 50, No. 9, 2152–2159, 2002.
11. Habib, M. A., M. Barkat, B. Aissa, and T. A. Denidni, "CA-CFAR detection performance of radar targets embedded in "non centered chi-2 Gamma" clutter," *Progress In Electromagnetics Research*, Vol. 88, 135–148, 2008.
12. Van Der Spek, G. A., "Detection of a distributed target," *IEEE Transactions on Aerospace and Electronics Systems*, Vol. 7, No. 5, 922–931, 1971.
13. Hughes, P. K., "A high-resolution radar detection strategy," *IEEE Transactions on Aerospace and Electronics Systems*, Vol. 19, No. 5, 663–667, 1983.
14. Gerlach, K., M. Steiner, and F. C. Lin, "Detection of a spatially distributed target in white noise," *IEEE Signal Processing Letters*, Vol. 4, No. 7, 198–200, 1997.
15. Gerlach, K. and M. J. Steiner, "Adaptive detection of range distributed targets," *IEEE Transactions on Signal Processing*, Vol. 47, No. 7, 1844–1851, 1999.
16. Conte, E., A. De Maio, and G. Ricci, "GLRT-based detection algorithms for range-spread targets," *IEEE Transactions on Signal Processing*, Vol. 49, No. 7, 1336–1348, 2001.
17. De Maio, A. and A. Farina, "Adaptive detection of range spread targets with orthogonal rejection," *IEEE Transactions on Aerospace and Electronics Systems*, Vol. 43, No. 2, 737–751, 2007.
18. Bandiera, F., A. De Maio, A. S. Greco, and G. Ricci, "Adaptive radar detection of distributed targets in homogeneous and partially homogeneous noise plus subspace interference," *IEEE Transactions on Signal Processing*, Vol. 55, No. 4, 1223–1237, 2007.
19. Gong, Q. and Z.-D. Zhu, "Study stap algorithm on interference target detect under non-homogenous environment," *Progress In Electromagnetics Research*, Vol. 99, 211–224, 2009.

20. Hao, C., F. Bandiera, J. Yang, D. Orlando, S. Yan, and C. Hou, "Adaptive detection of multiple point-like targets under conic constraints," *Progress In Electromagnetics Research*, Vol. 129, 231–250, 2012.
21. Wang, X., L. Jin, and J. Gao, "A study on detection algorithm for range-distributed targets in stepped-frequency radar," *Modern Radar*, Vol. 31, No. 5, 35–38, 2009.
22. Levanon, N., "Stepped-frequency pulse-train radar signal," *IEE Proceedings Radar, Sonar and Navigation*, Vol. 149, No. 6, 297–309, 2002.
23. Tian, B., D.-Y. Zhu, and Z.-D. Zhu, "A novel moving target detection approach for dual-channel SAR system," *Progress In Electromagnetics Research*, Vol. 115, 191–206, 2011.
24. Mao, X., D.-Y. Zhu, L. Wang, and Z.-D. Zhu, "Comparative study of RMA and PFA on their responses to moving target," *Progress In Electromagnetics Research*, Vol. 110, 103–124, 2010.
25. Wu, Z.-S., J.-P. Zhang, L.-X. Guo, and P. Zhou, "An improved two-scale model with volume scattering for the dynamic ocean surface," *Progress In Electromagnetics Research*, Vol. 89, 39–56, 2009.
26. Chua, M. Y. and V. C. Koo, "FPGA-based chirp generator for high resolution UAV SAR," *Progress In Electromagnetics Research*, Vol. 99, 71–88, 2009.
27. Li, D. and T. Long, "Target's redundancy removed algorithms of step frequency radar," *Acta Electronica Sinica*, Vol. 28, No. 6, 60–63, 2000.
28. Zhang, H., S. Zhang, and Q. Li, "Target extracting algorithm and system parameter design in stepped frequency modulated radar," *Acta Electronica Sinica*, Vol. 35, No. 6, 1153–1158, 2007.
29. Oppenheim, A. V. and R. W. Schafer, *Discrete-time Signal Processing*, 3rd Edition, Prentice-Hall, Inc., 2009.
30. Miller, K. S., *Multidimensional Gaussian Distributions*, Wiley, New York, 1964.